EXPERIMENTS ON THE EFFECT OF SWELL ON SCATTEROMETER RESPONSE

Brian K. Haus[1], Mark A. Donelan[1], William J. Plant[2], Olivier Troianowski[3]

(1) University of Miami, Rosenstiel School of Marine and Atmospheric Science, Division of Applied Marine Physics.
(2) University of Washington, Applied Physics Laboratory
(3) Sarnier & Associes, Nanterre Cedex, France

The reflection and scattering of microwave radiation from the sea surface is at the heart of satellite and airborne active remote sensing. Sensors carried on these platforms typically illuminate the sea surface with radiation in the microwave ranges of K_u band (2 – 3 cm) through L band (25 – 35 cm). At moderate to high incidence angles this radiation is most strongly backscattered to the sensor by ocean surface waves with wavelengths ~1/2 to 3/2 the microwave length. Radar systems respond not only to the energy density of the short surface waves but also to changes in the local incidence angle of the radiation and changes in the range to the surface. The short waves are generated and amplified by the wind and also respond to the hydrodynamic modulation of longer wind waves and swell. Keller and Wright (1975) demonstrated that the interaction between short waves and longer waves produced a modulation of microwave backscatter from a rough water surface. All of these modulating effects render long surface waves and other features visible to the radar.

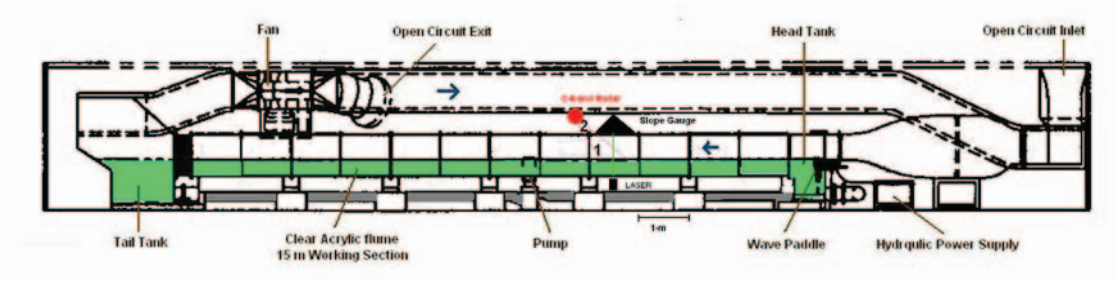

Figure 1. Schematic of the wind-wave tank showing the location of the elevation (1) and slope gauge (2) and radar dish (red).

Laboratory measurements to quantify the effect of long waves on the modulation of short waves and the effect that this modulation has on radar reflectivity have been conducted at the Air-Sea Interaction Saltwater Tank (ASIST) facility of the University of Miami (Figure 1). These experiments included direct observation of the modulation of short wave energy with long wave phase using non-intrusive techniques. The local water surface elevation and the slope vector were sampled using laser techniques at a point. The slope gauge uses two Fresnel lenses resting on glass supports and mounted back-to back to collect a wave-deflected laser beam in order to re-direct it towards the optical axis and to focus it onto a diffusing screen. The position of the beam on the

screen is proportional to the wave angular tilt. The laser spot on the screen is imaged onto a two-axis position sensor by means of a relay lens. The two-dimensional distribution of surface slopes were also imaged at a rate of 120 Hz using an optical imaging slope gauge (Figure 2).

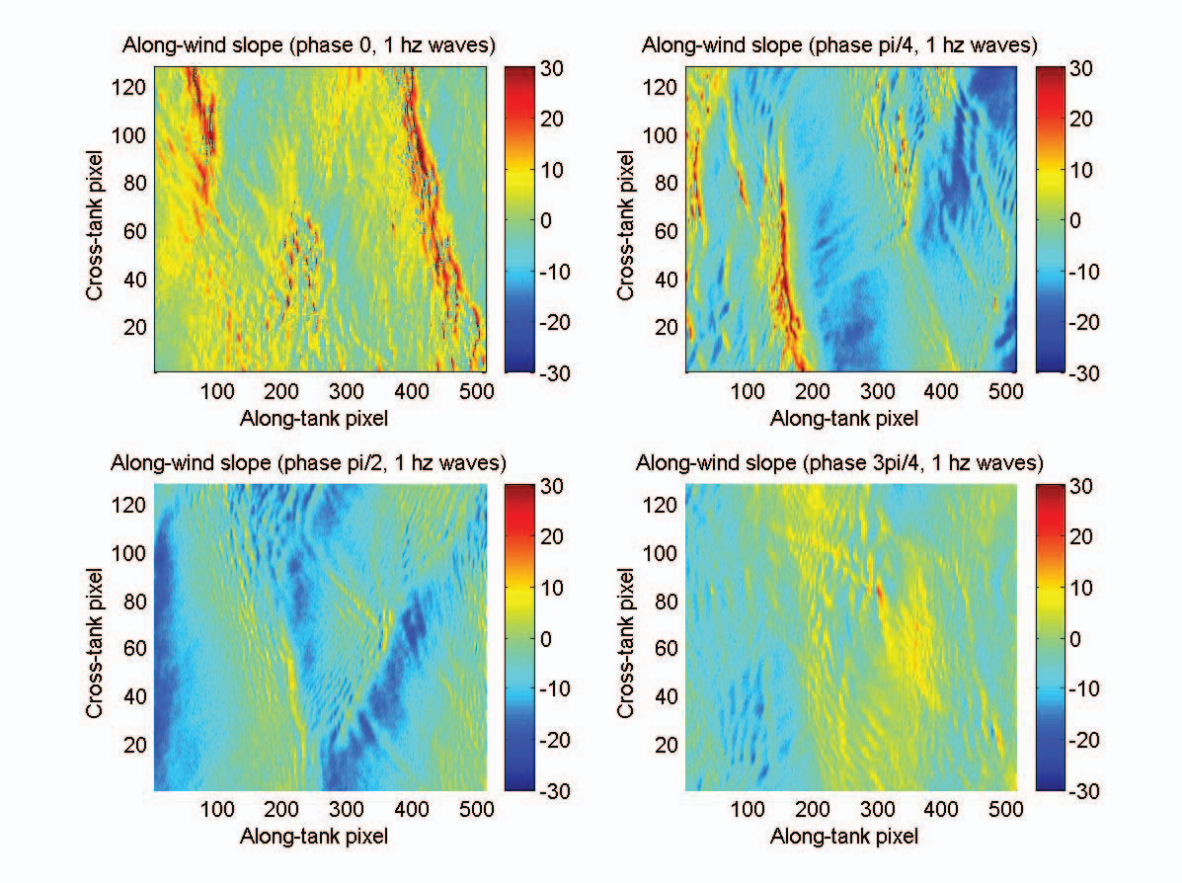

Figure 2. Snapshots of the surface slopes obtained from an optical imaging slope gauge with wind of 10 m/s (right to left as shown) at four phases of a 1-hz long wave also moving right to left. Total image size ~0.17 m crosstank x 0.34 m alongtank. Images obtained at a rate of 60 Hz. Slopes given in degrees.

Co-incident with these measurements, the radar backscatter was sampled over the same region of the surface using a dual-polarized C-band Doppler radar. The C-band radar emits both horizontal and vertical polarization signals, respectively at 5820 MHz and 5760 MHz with associated wavelengths of 5.15 cm and 5.21 cm. The radar antenna has been designed to focus at 1.8 meters in order to illuminate only the center area of the one meter wide tank. To define the illumination patterns over the test area and normalize the returned signal, the backscattered power from a suspended steel ball moving in the plane of incidence was measured (Figure 3). The radar returns were shown in an initial set of runs to be sensitive to reflections from the tank ceiling that were in phase with the long waves. Radar absorbing material was then installed in the roof of the tank to reduce these reflections. All measurements reported here were conducted with this absorbing material in place.

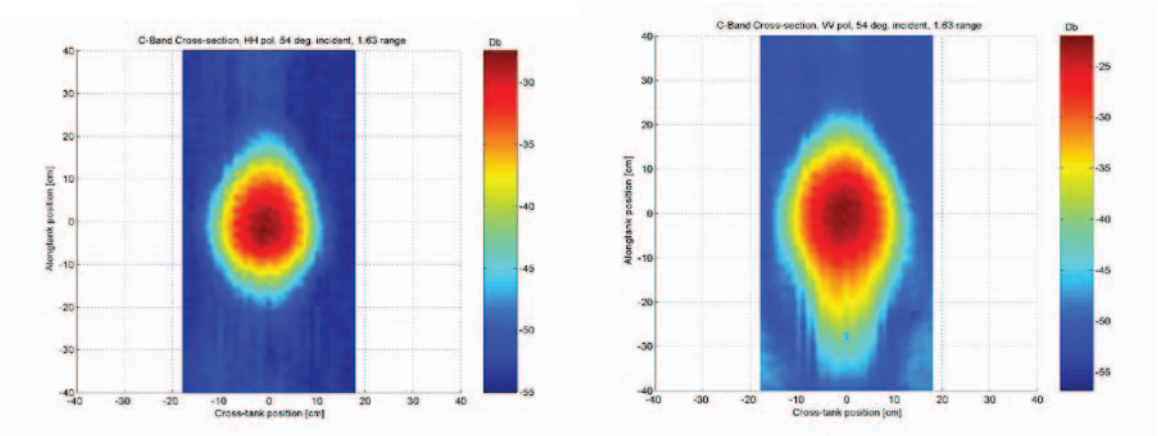

Figure 3. Normalized radar cross section patterns over the ASIST test section for an angle of incidence of 54 degrees at VV (left) and HH (right) polarization.

Experiments were run with various wind velocities modulated by mechanical long-waves of varying amplitude and frequency. The centerline wind speeds investigated were: 0, 5, 7.5, 10, 12.5, 15 m/s. The corresponding effective neutral wind speeds at a height of 10 m are: 0, 7.6, 12.2, 16.8, 22.1, 27.3 m/s. A paddle was operated at 0.5 Hz and 1.0 Hz, each at two amplitudes leading to four different long wave slopes as well as no paddle-generated conditions. Thus the experiment consisted of 30 trials and this was repeated a few days later for a total of 60 runs.

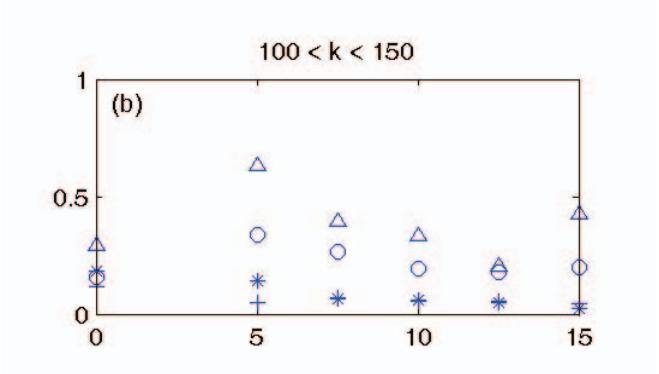

Figure 4. "Modulation amplitude" of the spectral density variations for the C-band wavenumber range (k~120) conditionally averaged on the fundamental of the paddle wave and normalized by the mean spectral density. The symbols correspond to different levels of slope amplitude of the paddle waves – (+; *a k ~ 0.018,* *; *a k ~ 0.034*, o; *a k ~ 0.075,* Δ*; a k ~ 0.134*) Figure reproduced from Donelan et al.(2009).

Donelan et al. (2010) reported on the hydrodynamic modulation of the short wind waves by the longer mechanical waves (Figure 4). They found that the addition of long paddle waves of various slopes reveals a strong interaction between the wind-sea and the long waves. Ultimately the steepest paddle waves (*ak ~ 0.1*) eliminated the peak enhancement of the wind-sea and reduced its saturation spectrum to the level of the equilibrium range. This effect of long waves on shorter waves explains the phenomenon of peak enhancement, in which the spectral density of a given wavenumber in a wind-generated sea is a maximum when that wavenumber is at the spectral peak. As the wavenumber moves above the spectral peak the longer waves modulate its spectral density driving it into breaking-limited saturation and therefore reducing its net spectral density. The mean spectral density of waves in the equilibrium range was insensitive to the long wave slope for moderate slopes. The oceanic modulation deduced by Hara and Plant (1994) from radar

backscatter data was found to be in good qualitative agreement with the directly observed hydrodynamic modulation in the laboratory (Donelan et al., 2010).

When there were no long waves, the short wave structure as observed by the 2-D slope gauge was well developed with peaks in surface slopes corresponding to the wavelength of the peak wind waves and having a clear group structure. This organization was in sharp contrast to the variability of the slopes observed when a 1 Hz mechanical long-wave was generated in the same direction as the wind waves. The slopes linked to the wind wave were suppressed, while there was modulation at the 1 Hz long-wave frequency. Significant modulation of the C-band HH polarized radar return was evident at the long wave frequency. The observed polarization ratios were consistent with the Bragg condition as predicted by the Valenzuela (1978) polarization ratio model at low wind speeds (Figure 5). As the wind speed increased the polarization ratio decreased, and the ratio of non-Bragg scattering to the total NRCS increased.

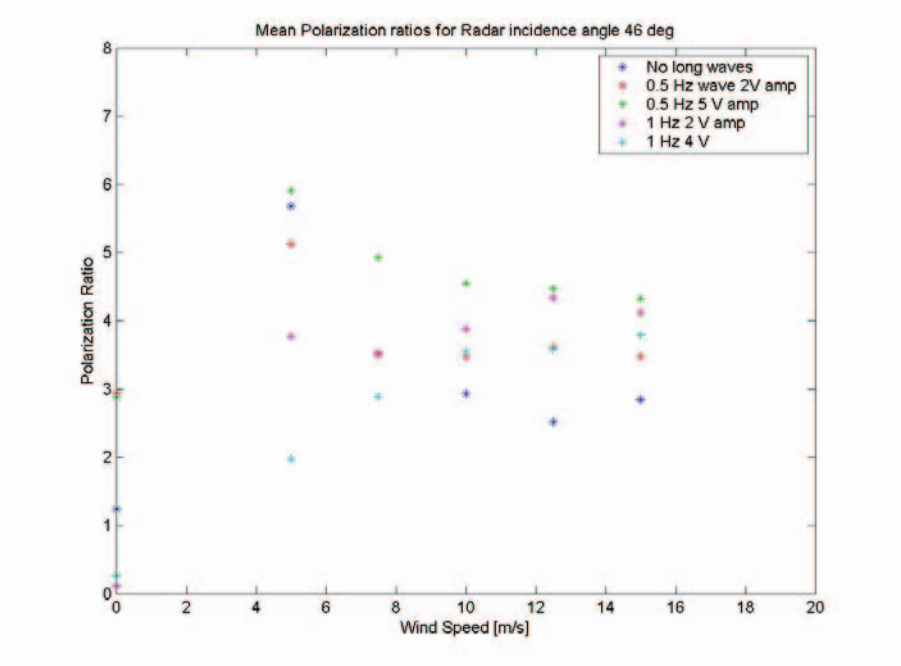

Figure 5. Polarization ratios vs wind speed for different combinations of long wave amplitudes and frequencies.

References

Donelan, M. A., B. K. Haus, W. J. Plant and O. Troianowski, (2010). The modulation of short wind waves by long waves. *J. Geophys. Res*., (accepted).

Hara, T. and W. J. Plant (1994), Hydrodynamic modulation of short wind-wave spectra by long waves and its measurement using microwave backscatter. *J. Geophys. Res*., 99 (C5), 9767-9784.

Keller, W.C. and J.W. Wright (1975), Microwave scattering and the straining of wind-generated waves, *Radio Science*, 10(2), 139-147.